Fluorophore-assisted light inactivation produces both targeted and collateral effects on N-type calcium channel modulation in rat sympathetic neurons

Juan Guo, Huanmian Chen, Henry L. Puhl III and Stephen R. Ikeda*

Section on Transmitter Signalling, Laboratory of Molecular Physiology, National Institute on Alcohol Abuse and Alcoholism, National Institutes of Health, Bethesda, MD 20892 USA

Fluorophore-assisted light inactivation (FALI) is a method to inactivate specific proteins on a time scale of seconds to minutes using either diffuse or coherent light. Here we examine a novel FALI modality that utilizes a fluorescein-conjugated polypeptide, α-bungarotoxin (BTX) and a 13 amino acid BTX-binding site engineered into the N-terminus of metabotropic glutamate receptor 8a (mGluR8a), a class C G-protein-coupled receptor (GPCR). The tagged mGluR8a was expressed in rat sympathetic neurons and labelled with fluorescein-conjugated BTX (FL-BTX). The efficacy of FALI was evaluated by monitoring mGluR8a-mediated inhibition of calcium currents (I_{Ca}) using whole-cell voltage-clamp techniques. Following either wide-field or laser illumination of FL-BTX-labelled neurons, mGluR8a-mediated I_{Ca} inhibition was greatly attenuated whereas holding current and basal I_{Ca}, measures of non-specific effects, were minimally affected. Sodium azide, a collision quencher of singlet oxygen, reduced the magnitude of FALI-mediated effects supporting a role for reactive oxygen species in the process. Although these results were consistent with an acute inactivation of mGluR8a, the intended target, two findings confounded this interpretation. First, effects on a natively expressed signalling pathway, α_2-adrenergic receptor-mediated I_{Ca} modulation, were observed following illumination of neurons expressing FL-BTX-labelled sodium channel β2 subunits or ionotropic 5-HT_3 receptors, proteins with no overt relationship to GPCR signalling pathways. Second, GPCR-independent I_{Ca} modulation induced with intracellular guanylyl imidophosphate was also attenuated by FALI. These data challenge the assumption that the fluorophore-tagged protein is the sole target of FALI and provide evidence that collateral damage to proximal proteins occurs following fluorophore illumination.

(Received 5 May 2006; accepted after revision 25 July 2006; first published online 27 July 2006)

Corresponding author S. R. Ikeda: Laboratory of Molecular Physiology, National Institute on Alcohol Abuse and Alcoholism, 5625 Fishers Lane, Room TS-06, MSC 9411, Bethesda, MD, 20892-9941 USA. Email: sikeda@mail.nih.gov

A common approach to understanding signalling cascades involves deletion of a specific component followed by analysis of the resulting phenotype. Although genetic technologies such as inducible gene knockout in mice, antisense DNA and, more recently, small interfering RNA, have advanced our understanding of signalling pathways, these techniques require waiting for the endogenous targeted protein to turnover. During this period, compensatory changes can occur which confound interpretation. Hence, a technique targeting the protein rather than the synthetic mechanism would be beneficial.

Fluorophore-assisted light inactivation (FALI) is a technique in which a fluorophore is attached to a targeted protein either directly or indirectly via a labelled intermediate (Eustace & Jay, 2003). Following illumination, energy is transferred from the fluorophore to oxygen molecules resulting in the generation of reactive oxygen species (ROS) such as singlet oxygen ($^1O_2$). The ROS reacts with amino acids in close proximity to the fluorophore producing functional inactivation through incompletely understood mechanisms (Davies, 2003). An advantage of FALI is that protein inactivation is a rapid process, occurring within seconds to minutes, thus eliminating the possibility of functional compensation arising from newly synthesized proteins. Additionally, the ability to tightly focus light facilitates targeting inactivation to discrete cellular compartments.

Several alternative modalities of FALI have evolved (see review by Tour, 2005). In the original studies of Jay and colleagues (Jay, 1988; Linden *et al.* 1992; Liao *et al.* 1994), termed chromophore-assisted laser inactivation (CALI), antibodies labelled with malachite green were

 DOI: 10.1113/jphysiol.2006.113068

used to inactivate proteins following laser illumination. The process was spatially restricted (half-maximal radius of inactivation ∼1.5 nm), *independent* of molecular oxygen and proposed to be mediated by hydroxyl radicals. Problems with limited solubility and the requirement for high intensity pulsed laser illumination have limited widespread adoption of CALI. Recently, protein inactivation based on illumination of fluorophores (fluorescein, derivatives of fluorescein and fluorescent proteins) has been reported. FALI, unlike CALI, requires molecular oxygen and is believed to arise from $^1O_2$ generation (Eustace & Jay, 2003; Horstkotte *et al.* 2005). The half-life of $^1O_2$ is greater than hydroxyl radicals and accordingly, the radius of action potentially greater. Several modalities to bring the fluorophore proximal to the targeted protein have been developed including membrane-permeable biarsenical fluorophores (FlAsH and ReAsH) that bind a tetracysteine motif (Tour *et al.* 2003), fusion of fluorescent proteins (Rajfur *et al.* 2002; Tanabe *et al.* 2005) and fusion of a receptor (FKBP12(F36V)) for an engineered high affinity ligand (SLF; Marks *et al.* 2004). Although inactivation of the targeted protein was demonstrated in these studies, specificity in the context of a tightly coupled neuronal signalling pathway has not been explored in detail.

We therefore tested whether FALI disrupts N-type ($Ca_V2.2$) Ca^{2+} channel inhibition mediated by metabotropic glutamate receptor type 8a (mGluR8a) heterologously expressed in sympathetic neurons (Guo & Ikeda, 2005). The signalling pathway in this model system consists of tightly coupled membrane-delimited components: G-protein-coupled receptor (GPCR), heterotrimeric G-protein and Ca^{2+} channels thus allowing scrutiny of potential collateral effects. Fluorescein-conjugated α-bungarotoxin (BTX) was used to label mGluR8a with a high affinity pharmacotope (Sekine-Aizawa & Huganir, 2004; McCann *et al.* 2005) engineered into the extracellular N-terminus and protein inactivation accomplished with both wide-field and laser illumination. The specificity of FALI-mediated disruption of mGluR8a signalling was determined using whole-cell voltage-clamp recordings.

Methods

BTX-binding-site fusion constructs

A cDNA construct comprised of mGluR8a containing an extracellular α-bungarotoxin binding site (BBS) was made by inserting an *Nru*I site at residue 34 beyond the predicted signal sequence of mGluR8a (GenBank: AY673682; Guo & Ikeda, 2005) in the pEGFP-N1 vector. The EGFP coding sequence was deleted using QuikChange mutagenesis (Stratagene, La Jolla, CA, USA) before insertion of the BBS tag. Oligonucleotide pairs (5′-ATCTCCGGATGGAGATACTACGAGAGCTCCCTGGAGCCCTACCCTGACGGCGGAGGA-3′ and complement 5′-TCCTCCGCCGTCAGGGTAGGGCTCCAGGGAGCTCTCGTAGTATCTCCATCCGGAGAT-3′) encoding a BBS tag with a four-glycine linker (WRYYESSLEPYPDGGGG) were annealed and then ligated into the *Nru*I site.

The voltage-gated Na^+ channel $\beta2$ subunit ($Na_V\beta2$; GenBank: NM˙012877) was amplified from rat whole brain cDNA (BD Biosciences Clontech, Palo Alto, CA, USA) using *PfuUltra* (Stratagene) polymerase with the following primers: 5′-GATCCTCGAGCCACCATGCACAGGGATGCCTGGCTACC-3′ and 5′-GATCGCGGCCGCTTAAAGCTTCTTGGCGCCATCTTCCGC-3′ and the product ligated into pCI vector (Promega, Madison, WI, USA). An *Eco*RV site was inserted into $Na_V\beta2$ after the predicted signal sequence at residue 34 using QuikChange mutagenesis. This construct was digested with *Eco*RV and the 13 amino acid BTX binding site was incorporated by annealing and ligation of the following oligonucleotides: 5′-ATCTCCGGATGGAGATACTACGAGAGCTCCCTGGAGCCCTACCCTGACGGCGGAGA-3′ and complement 5′-TCCTCCGCCGTCAGGGTAGGGCTCCAGGGAGCTCTCGTAGTATCTCCATCCGGAGAT-3′. A 5-HT_3 receptor cDNA, in the vector pcDNA3.1 (Invitrogen, Carlsbad, CA, USA), containing two tandem BBSs added to the extracellular C-terminus (5-HT_3R–2BBS) was a gift from Dr David Lovinger (NIH/NIAAA, Bethesda, MD, USA). All constructs were sequenced using a CEQ 8000 Automated DNA Sequencer (Beckman-Coulter, Fullerton, CA, USA).

Neuron isolation and microinjection of cDNA

The procedures for enzymatic dissociation of rat superior cervical ganglion (SCG) neurons and intranuclear microinjection of cDNA have been previously described (Ikeda, 2004; Ikeda & Jeong, 2004). Briefly, adult male Wistar rats were decapitated after anaesthesia with CO_2 inhalation as approved by the Institutional Animal Care and Use Committee. Bilateral SCG were desheathed, cut into small pieces and then transferred into modified Earle's balanced salt solution (EBSS) containing collagenase D (0.7 mg ml^{-1}, Roche, Indianapolis, IN, USA), trypsin (0.3 mg ml^{-1}, Worthington Biochemical Corporation, Freehold, NJ, USA) and DNase I (0.05 mg ml^{-1}, Sigma, St Louis, MO, USA). After 1 h incubation in a shaking water bath at 36°C, SCG fragments were shaken vigorously to release the neuronal somata. The dissociated neurons were washed and resuspended in minimum essential medium (MEM) containing 10% fetal calf serum, 100 U ml^{-1} penicillin and 100 mg ml^{-1} streptomycin (Invitrogen), plated onto poly L-lysine-coated tissue culture dishes (35 mm) and placed in a 5% CO_2 incubator at 37°C.

Mammalian expression vectors pCI, pcDNA3.1 and pEGFP-N1 (BD Biosciences Clontech) containing

inserts encoding wild type mGluR8a (wt-mGluR8a), BBS–mGluR8a, BBS–$Na_V\beta2$, 5-HT_3R–2BBS were stored at −20°C as ∼1 μg μl^{-1} stock solution in TE buffer (10 mM Tris, 1 mM EDTA, pH 8). A FemtoJet 5247 microinjection unit and 5171 micromanipulator (Eppendorf, Madison, WI, USA) controlled with custom-designed software were used to inject DNA at a pipette concentration of 100–200 ng μl^{-1}. A construct expressing monomeric red fluorescence protein (Campbell *et al.* 2002; a gift from Dr Roger Y. Tsien, University of California, San Diego, CA, USA) fused to three copies of the SV40 large T-antigen nuclear localization signal (pRFP-nuc; 5–10 ng μl^{-1}) was co-injected to facilitate identification of expressing neurons.

HEK 293 cell culture and transfection

HEK 293 cells were cultured in MEM supplemented with 10% fetal calf serum, 100 U ml^{-1} penicillin and 100 mg ml^{-1} streptomycin. The cells, at ∼95% confluence, were transfected with cDNAs as follows. A mixture of 1 μg of BBS–mGluR8a, 0.1 μg pEGFP-N1 and 4 μl of fully deacylated (Thomas *et al.* 2005) polyethylenimine (7.5 mM) was made in 100 μl of Opti-MEM (Invitrogen) and incubated for 20 min. The mixture was then added to a cell culture dish containing HEK 293 cells.

BTX binding and imaging

After 16–24 h, HEK 293 cells or SCG neurons expressing BBS-tagged constructs were labelled with 50 ng ml^{-1} (∼6 μM) of either fluorescein-, tetramethylrhodamine- or Alexa Fluor 488-conjugated BTX (Molecular Probes, Eugene, OR, USA) in Dulbecco's phosphate-buffered saline (without Ca^{2+} and Mg^{2+}) at room temperature (22–26°C) for 30 min and then washed four times with the buffered saline to remove unbound BTX. The labelled cells were observed with a Nikon Eclipse TE2000 inverted fluorescence microscope equipped with a 60 × 1.4 NA objective. HEK 293 cells and SCG neurons were imaged using a cooled CCD camera (Orca ERG, Hamamatsu, Japan) and Openlab software (Improvision Inc., Lexington, MA, USA).

Electrophysiological recordings

As previously described (Guo & Ikeda, 2005), Ca^{2+} channel currents (I_{Ca}) were recorded from rat SCG neurons using the whole-cell patch-clamp technique. Custom-designed software (S5) was used for voltage protocol generation and data acquisition through an ITC-18 data acquisition interface (InstruTECH, Port Washington, NY, USA). I_{Ca} traces were analog filtered at 1 or 2 kHz (−3dB, 4-pole Bessel) and digitized at 10 kHz. All recording were performed at room temperature. A double-pulse protocol consisting of two 25 ms depolarization pulses to +10 mV separated by a 50 ms conditioning pulse to +80 mV (Elmslie *et al.* 1990) was used to elicit I_{Ca}.

The external recording solution contained (mM): 140 methanesulphonic acid, 145 tetraethylammonium hydroxide (TEA-OH), 10 Hepes, 10 glucose, 10 $CaCl_2$; and 0.0003 tetrodotoxin (TTX), pH 7.4 with TEA-OH. The internal (pipette) solution contained (mM): 120 *N*-methyl-D-glucamine, 20 TEA-OH, 11 EGTA, 10 Hepes, 10 sucrose, 10 HCl, 1 $CaCl_2$, 4 MgATP, 0.3 Na_2GTP and 14 Tris creatine phosphate, pH 7.2 with methanesulphonic acid. The osmolalities of the bath and pipette solutions were adjusted with sucrose to 325 and 300 mosmol kg^{-1}, respectively.

Light sources for FALI

Two light sources were used for the FALI experiments. In early experiments, a standard epi-illumination source consisting of a 100 W Hg arc lamp, EGFP filter cube (excitation D480/10) and Nikon 40 × 0.7 NA CFI60 phase contrast objective was used. In later experiments, the 488 nm line from an argon ion laser (salvaged from an old Olympus FluoView confocal microscope) was launched via a Zeiss 5 × 0.15 NA Plan Neofluar objective into a 0.22 NA 105 μm step index multimode optical fibre (AFS105/125Y, ThorLabs, Inc., Newton, NJ, USA). The fibre was positioned using a flexure stage and illumination duration controlled by a laser shutter system (both from ThorLabs). On exit from the optical fibre, laser power was 1.6 mW as determined with a selectable wavelength power meter (Ophir Optronics, Wilmington, MA, USA). The optical fibre was passed through a glass microelectrode blank and aligned near the neuron somata with a micromanipulator.

Data analyses and statistics

I_{Ca} was analysed using Igor Pro software (WaveMetrics, Lake Oswego, OR, USA). All data were expressed as mean ± S.E.M. I_{Ca} inhibition (%) was determined as $(I_{con} - I_{agonist})/I_{con} \times 100$, where I_{con} and $I_{agonist}$ are the prepulse I_{Ca} before and after agonist application. The prepulse and postpulse I_{Ca} were measured isochronally 10 ms after initiation of the test pulse (+10 mV). Facilitation ratio was calculated as the ratio of postpulse to prepulse I_{Ca} in the absence (basal facilitation ratio) or presence of agonist. The holding currents at −80 mV were measured at 5 ms after initiation of the double-pulse protocol. Statistical comparisons were determined (Prism, GraphPad Software, San Diego, CA, USA) using the unpaired and paired *t* test, one-way ANOVA followed by Newman-Keuls test, Kruskal-Wallis followed by Dunn's test or Pearson correlation, as appropriate. Non-linear least-squares curve fitting was performed using a Marquardt-Levenberg algorithm (Igor Pro). $P < 0.05$ was considered significant.

Results

Expression and labelling of BBS-mGluR8a in HEK 293 cells and rat SCG neurons

Metabotropic glutamate receptors, members of the class C family of G-protein-coupled receptors (GPCR), have a large *N*-terminal extracellular domain that contains the binding region (LBR) for the endogenous ligand, L-glutamate (L-Glu). A 13-aa peptide derived from the nicotinic acetylcholine receptor that binds BTX with high affinity (BBS) was introduced into mGluR8a just distal to the predicted signal sequence to facilitate live cell labelling with commercially available fluorophore-conjugated BTX (Sekine-Aizawa & Huganir, 2004; McCann *et al.* 2005). This strategy has several potential advantages for targeting mGluR8a using FALI. First, high resolution structure of the mGluR1a extracellular domain (Kunishima *et al.* 2000) indicates close proximity of the LBR to the predicted location of the BBS (ca 20–30 Å). Second, BTX is a small polypeptide (74 residues) when compared with fluorophore-labelled IgG (used in many previous FALI studies) and thus proximity of the fluorophore to the intended target should be improved. Finally, structural data allow the topography of the mGluR extracellular domain in relationship to the plasma membrane to be inferred (Fig. 1*A*; Kunishima *et al.* 2000). The bulk of the LBR is predicted to distance the BBS and hence fluorophore, from the plasma membrane and

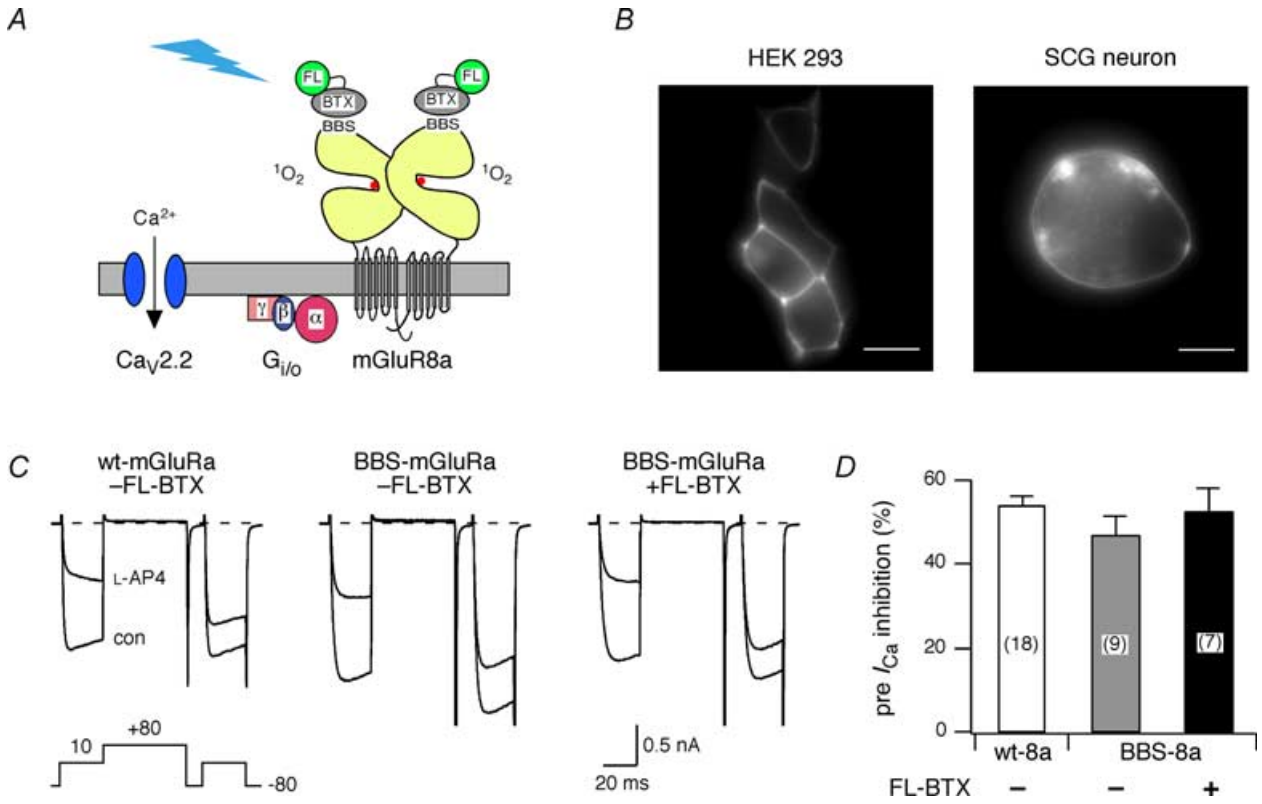

Figure 1. Expression and labelling of BBS-mGluR8a in HEK 293 cells and rat sympathetic neurons
A, conceptual schematic of fluorophore-assisted light inactivation (FALI). Fluorescein-conjugated α-bungarotoxin (FL–BTX) selectively binds to the bungarotoxin binding site (BBS) inserted near the ligand-binding domain of mGluR8a. Illumination of the conjugated fluorescein generates singlet oxygen ($^1O_2$) that inactivates mGluR8a and subsequently disrupts N-type Ca^{2+} channel ($Ca_V2.2$) inhibition mediated via $G\beta\gamma$ subunit. *B*, fluorescence images (60 × 1.4 NA objective) of HEK 293 cells (left) and rat superior cervical ganglion (SCG) neurons (right) expressing BBS-tagged mGluR8a and following labelling (live cells, room temperature) with tetramethylrhodamine (HEK 293 cell) or Alexa Fluor 488 (SCG neuron) conjugated BTX. The 'rim-type' fluorescence pattern indicates plasma membrane expression of mGluR8a. Horizontal scale bar is 10 μm. *C*, superimposed Ca^{2+} channel current (I_{Ca}) traces recorded in the absence (con) or presence (L-AP4) of 1 μM L-AP4 from a neuron expressing wt-mGluR8a (left), BBS–mGluR8a (centre), or BBS–mGluR8a and labelled with FL–BTX (right). Currents were evoked with the voltage protocol illustrated (bottom left). The dashed lines indicate the zero current level. I_{Ca} traces were *not* leak subtracted here or in subsequent figures. *D,* summary bar graph of mean ± S.E.M. I_{Ca} inhibition by L-AP4 (1 μM) from neurons expressing wt-mGluR8a (open bar), BBS-tagged mGluR8a without (grey bar) and with FL–BTX labelling (filled bar). I_{Ca} inhibition was measured 10 ms after initiation of the test pulse (+10 mV) in the absence or presence of L-AP4. The number of neurons tested, here and in subsequent figures, is indicated in parentheses.

other components (e.g. heterotrimeric G-proteins and N-type Ca^{2+} channels) of the signalling cascade. Structural and biochemical data (Kniazeff *et al.* 2004) indicate that mGluRs exist as homodimers as indicated in the schematic (Fig. 1*A*).

The expression pattern of BBS–mGluR8a was examined following transfection in HEK 293 cells or injection into the nucleus of rat SCG neurons. Plasmids encoding fluorescent proteins (pEGFP or pRFP-Nuc) were co-introduced to identify successfully transfected or injected cells. Following 16–24 h incubation at 37°C, living cells were labelled at room temperature with fluorophore-conjugated BTX (fluorescein, Alexa Fluor 488, or tetramethylrhodamine) and observed with fluorescence microscopy. Figure 1*B* shows the expression and labelling of the BBS–mGluR8a with tetramethylrhodamine- and Alexa Fluor 488-conjugated BTX in HEK 293 cells (left panel) and rat SCG neurons (right panel), respectively. The 'rim-type' fluorescence pattern clearly indicates plasma membrane expression of mGluR8a. The BTX labelling was highly selective, only transfected or injected cells were labelled with BTX (data not shown). Although the fluorescence intensity attenuated with time, the fluorescence was still detectable 1 h after washout of BTX.

Insertion of the BBS and labelling with FL-BTX did not affect mGluR8a function

To determine whether the insertion of the BBS tag or binding of BTX altered receptor function, BBS–mGluR8a was expressed in rat SCG neurons and mGluR8a-mediated I_{Ca} modulation was compared with a previous study of wt-mGluR8a (Guo & Ikeda, 2005). I_{Ca} in SCG neurons is primarily ω-conotoxin GVIA-sensitive N-type Ca^{2+} current (Ikeda, 1991). Previously we have demonstrated that functional metabotropic glutamate receptors are not expressed on the soma of rat SCG neurons (Ikeda *et al.* 1995; Kammermeier & Ikeda, 1999; Guo & Ikeda, 2005) thus assuring that responses arose from heterologously expressed receptors. Figure 1*C* illustrates the effects of L-(+)-2-amino-4-phosphonobutyric acid (L-AP4; 1 μM), a selective group III mGluR agonist, on I_{Ca} elicited from SCG neurons previously injected with mGluR8a cDNA. I_{Ca} was elicited from a holding potential of −80 mV with a voltage protocol (Fig. 1*C*, below left panel) consisting of two 25 ms depolarization pulses to +10 mV separated by a 50 ms conditioning pulse to +80 mV (Elmslie *et al.* 1990). The prepulse and postpulse I_{Ca}s were measured isochronally at 10 ms from the beginning of the test pulse. Two parameters of inhibition were measured, prepulse I_{Ca} inhibition and facilitation ratio. The latter is defined as the ratio of the postpulse to prepulse I_{Ca} amplitude and is a hallmark of voltage-dependent inhibition mediated by G$\beta\gamma$ (Herlitze *et al.* 1996; Ikeda, 1996; Ikeda & Dunlap, 1999).

In rat SCG neurons injected with a cDNA encoding wt-mGluR8a, L-AP4 inhibited prepulse I_{Ca} by 54 ± 2% (n = 18; Fig. 1*C*, left and 1*D*). Similarly, 1 μM L-AP4 inhibited I_{Ca} by 48 ± 5% (n = 9) in the BBS–mGluR8a-expressing neurons (Fig. 1*C*, middle and 1*D*), which was not significantly different from the wt-mGluR8a-expressing neurons, suggesting that insertion of a BBS tag did not alter the function of mGluR8a, i.e. the coupling of mGluR8a to N-type Ca^{2+} channels. Following labelling of BBS–mGluR8a-expressing neurons with fluorescein-conjugated BTX (FL–BTX), prepulse I_{Ca} inhibition was unchanged (52 ± 6%, n = 7; Fig. 1*C*, left and 1*D*). Likewise, the facilitation ratio in the presence of L-AP4 was similar for all three conditions (1.9 ± 0.1, 1.9 ± 0.2 and 2.1 ± 0.2, respectively). Therefore, neither insertion of the BBS tag nor BTX labelling altered mGluR8a-mediated Ca^{2+} channel modulation.

FALI using wide-field illumination

The effects of wide-field illumination (100 W Hg lamp, EGFP filter cube, 40 × 0.7 NA objective) on I_{Ca} modulation are illustrated in Fig. 2 and summarized in Fig. 3. Four parameters were monitored during these experiments: (1) leak or holding current (at −80 mV) to assess non-specific actions on plasma membrane integrity, (2) basal (i.e. in the *absence* of agonist) prepulse I_{Ca} amplitude changes to assess direct effects on N-type Ca^{2+} channels, (3) agonist-mediated prepulse I_{Ca} inhibition to assess receptor function, and (4) facilitation ratio (in the *presence* of agonist) to assess mechanism of modulation (i.e. voltage-dependent *versus* -independent inhibition).

In the absence of FL–BTX labelling, wide-field illumination had little effect on the function of BBS–mGluR8a. I_{Ca} was evoked at 0.1 Hz with the previously described voltage protocol from neurons expressing BBS–mGluR8a (Fig. 2*A* and *B*). The first application of agonist (L-AP4; Fig. 2*A* and *B*; filled bar and trace labelled '1') produced a robust voltage-dependent modulation of I_{Ca} as indicated by the decrease in prepulse amplitude (Fig. 2*A* and *B*; filled circles) and increase in facilitation ratio (Fig. 2*A*, open squares). Following agonist washout, the neuron was continuously exposed to light (480 ± 10 nm; Fig. 2*A*, open bar) via the microscope objective and agonist applications repeated at several minute intervals (filled bars). A current trace acquired approximately 5 min into the illumination epoch (Fig. 2*B*, lower trace) revealed little change in holding current (Fig. 2*A* and *B*, open triangles), basal I_{Ca} properties or modulation. Illumination for 3 or 6 min produced only minor decreases (9 and 16%, respectively) in mean

normalized (to I_{Ca} amplitude prior to illumination) prepulse I_{Ca} amplitude (Fig. 3*A*, open bars) and negligible changes in mean holding current (< 2 pA, Fig. 3*B*, open bar). Agonist-mediated modulation assessed from prepulse I_{Ca} inhibition (normalized to inhibition prior to illumination; Fig. 3*C*, open bars) and facilitation ratio (Fig. 3*D*, open bars) was little changed at 3 min of illumination. After 6 min of illumination, decreases in both parameters were observed consistent with a rundown of agonist response during prolonged whole-cell recordings.

A similar experiment is illustrated in Fig. 2*C–D* with the exception that the neuron was incubated with FL–BTX prior to the recording. Here, agonist modulation after 3 min of illumination (Fig. 2*C* and *D*, labelled '2') was attenuated compared with the initial, pre-illumination, response (Fig. 2*C* and *D*, labelled '1'). Successive applications of agonist (Fig. 3*C*, filled bars) at about 3 min intervals resulted in decreasing amounts of modulation. The presence of fluorophore had virtually no effect on basal prepulse I_{Ca} amplitude at 3 or 6 min of illumination (Fig. 3*A*, filled bars) and only a small effect on holding current (mean change at 3 min was -12 ± 6 pA, $n = 7$). In contrast, prepulse I_{Ca} inhibition decreased to 0.50 ± 0.10 ($n = 3$) and 0.39 ± 0.07 ($n = 5$) of pre-illumination values, respectively, following 3 or 6 min of illumination (Fig. 3*C*, filled bars). Mean facilitation ratio also decreased following illumination (Fig. 3*D*, open bars) consistent with a decrease in voltage-dependent modulation.

Taken together, these data show that illumination of fluorophore-tagged mGluR8a results in a loss of I_{Ca} modulation consistent with receptor inactivation. The effects were fluorophore dependent and specific for the modulatory pathway. However, the duration of illumination required (several minutes) and magnitude

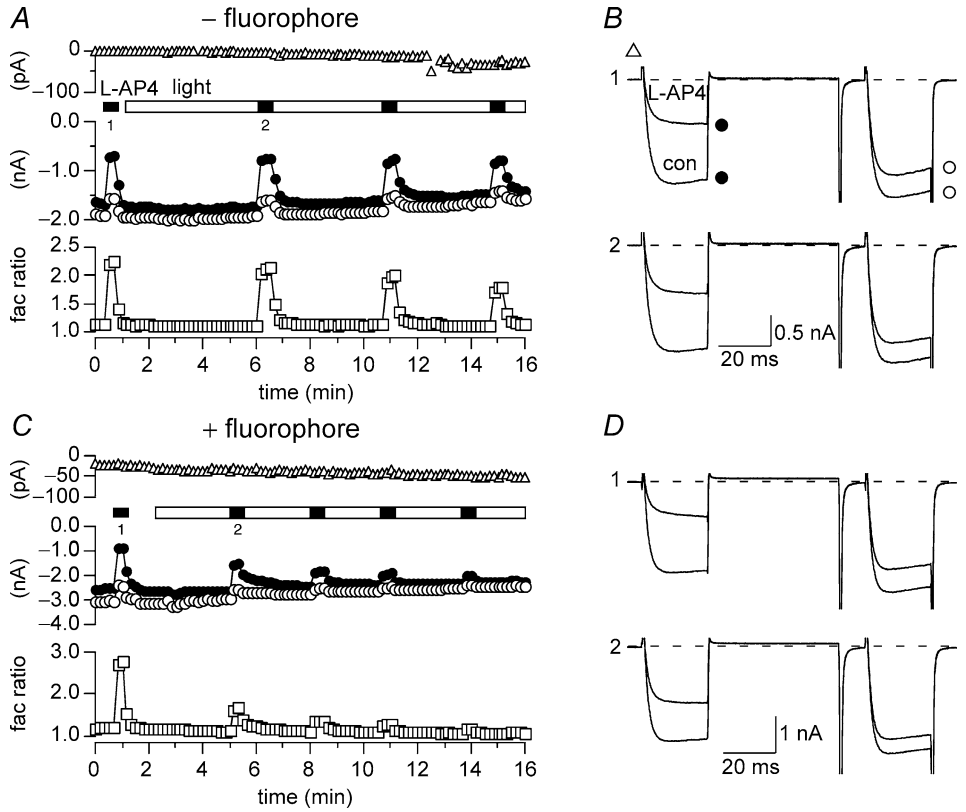

Figure 2. Wide-field illumination disrupted the function of BBS-mGluR8a with FL-BTX labelling
A and *C,* time course of the holding current (△), I_{Ca} amplitudes (open and filled circles) and facilitation ratio (open squares) for BBS–mGluR8a-expressing neurons in the absence (*A*) or presence (*C*) FL–BTX labelling. The currents were evoked every 10 s. The holding currents at −80 mV were measured at 5 ms after initiation of the double pulse protocol (bottom of the left panel of Fig. 1*C*). The prepulse (●) and postpulse (○) I_{Ca} amplitudes were measured 10 ms after initiation of the test pulse (+ 10 mV). Facilitation ratio was calculated as the ratio of postpulse to prepulse I_{Ca} amplitude. The open bar indicates the period of wide-field illumination and the filled bars indicate L-AP4 (1 μM) applications. *B* and *D,* superimposed I_{Ca} traces evoked in the absence (bottom trace) or presence (top trace) of L-AP4 recorded from neurons expressing BBS–mGluR8a. I_{Ca} traces in *B* and *D* correspond to the indicated time points in *A* and *C*, respectively. The upper (1) and (2) lower sets of I_{Ca} traces were obtained before and after illumination, respectively.

of disruption (~50%) led us to try more intense sources of light.

Laser illumination accelerated FALI

To increase the rate and efficacy of FALI, neurons were illuminated with the 488 nm line from an Ar ion laser. The laser output was coupled to a multimode optical fibre positioned near the neuron somata with a micromanipulator. The laser was adjusted to minimum output resulting in 1.6 mW of power measured on exit from the fibre. There were several advantages to the laser system compared with using a higher NA (i.e. oil) objective to deliver more light. First, fibre illumination allowed the use of 20 × low NA (i.e. dry) phase contrast objectives which was preferred for assessing neuronal health and the convenience of placing recording electrodes and perfusion devices. Second, high NA objectives concentrate light in the *z*-axis, hence uniform illumination of entire SCG neurons (~20–30 μm diameter) was potentially problematic. Third, laser illumination afforded higher power and greater control of duration.

To test whether application of FL–BTX in the absence of BBS–mGluR8a causes I_{Ca} inhibition after laser illumination, neurons injected with wt-mGluR8a were preincubated with FL–BTX, and the FALI effect was examined. As expected, 10 s laser illumination did not affect wt-mGluR8a-mediated I_{Ca} inhibition in the presence of preincubation with FL–BTX (Fig. 4*A* and *B*). Application of L-Glu (100 μM) inhibited I_{Ca} by 63 ± 4 and 62 ± 4%, before and after illumination ($n = 5$), respectively.

In Fig. 4*A*, laser illumination (open bar) for 10 s (per exposure period) did not affect mGluR8a-mediated I_{Ca} inhibition in the absence of preincubation with FL–BTX. Application of L-Glu inhibited I_{Ca} by 46 ± 7 and 43 ± 7%, before and after illumination ($n = 6$; Fig. 4*C*, filled circles; Fig. 5*C*, open bar), respectively. As with wide-field illumination in the absence of fluorophore, no overt changes in basal prepulse I_{Ca} amplitude (Fig. 5*A*, open bar) or holding current (Fig. 4*C*, open triangles; Fig. 5*B*, open bar) were observed. I_{Ca} traces, illustrated in Fig. 4*D*, acquired prior to (top) and after (bottom) 10 s of laser illumination revealed robust agonist-induced facilitation that was similar for both conditions (Fig. 4*C*, open squares; Fig. 5*D*, left bar).

Following FL–BTX treatment of BBS–mGluR8s-expressing neurons, 10 s of laser illumination produced a small decrease in basal prepulse I_{Ca} amplitude (Fig. 4*E*, filled circles; Fig. 5*A*, right bar, mean 11 ± 1%,

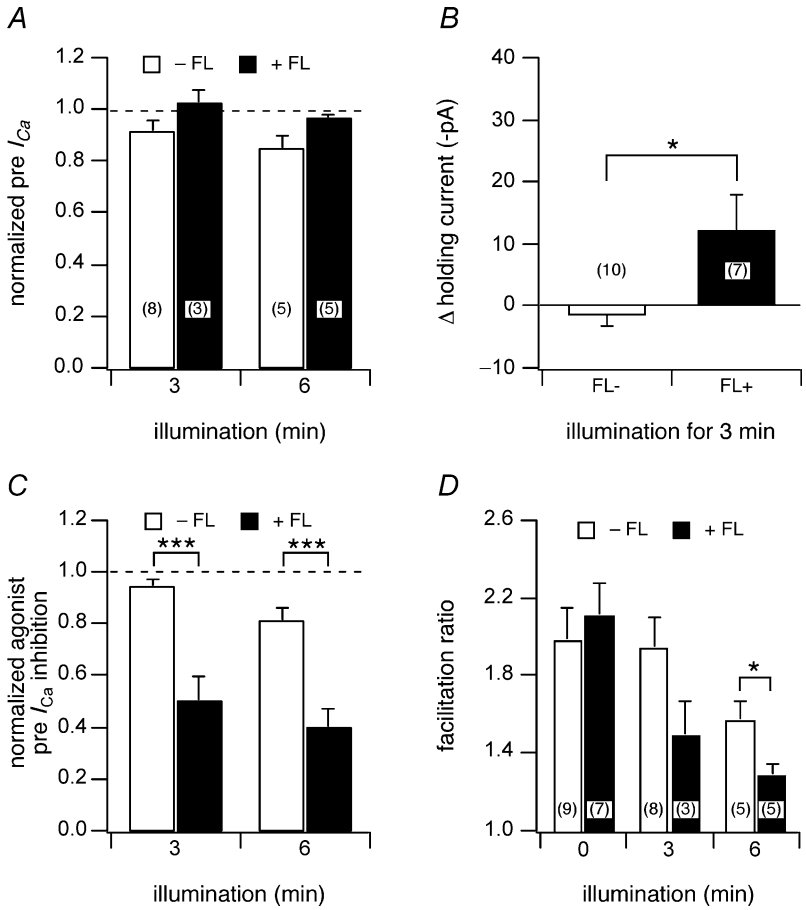

Figure 3. Wide-field illumination of BBS-mGluR8a resulted in a loss of I_{Ca} modulation without disrupting membrane integrity
A, the effect of 3 or 6 min illumination on normalized prepulse I_{Ca} in the absence or presence of FL–BTX labelling in BBS–mGluR8a-expressing neurons. I_{Ca} was normalized to the current before illumination. *B*, the effect of 3 min illumination on the holding current at −80 mV. The change of the holding current was calculated as the difference of the holding current before and after illumination. *C*, the effect of 3 or 6 min illumination on L-AP4 (1 μM) induced prepulse I_{Ca} inhibition in the absence or presence of FL–BTX labelling. The agonist-induced prepulse I_{Ca} inhibition was normalized to the inhibition before illumination. *D*, the effect of illumination on facilitation ratio in the absence or presence of FL–BTX labelling. The open and filled bars indicate the parameters in the absence or presence of FL–BTX labelling, respectively. $^*P < 0.05$, $^{***}P < 0.001$ compared with non-labelled neurons.

$n = 19$; $P < 0.05$ when compared with fluorophore). There was also an associated change in holding current (Fig. 4*E*, open triangles) that was quite variable among the cells tested (Fig. 5*B*, right bar, mean increase of 21.7 ± 7 pA, $n = 19$; $P < 0.05$ when compared with no fluorophore). Laser illumination significantly attenuated mGluR8a-mediated I_{Ca} modulation (Fig. 4*F*). Prepulse I_{Ca} inhibition fell to 0.40 ± 0.05 ($n = 19$; Fig. 5*C*, filled bar) of preillumination levels and facilitation ratio in the presence of agonist (L-Glu, 100 μM) decreased from

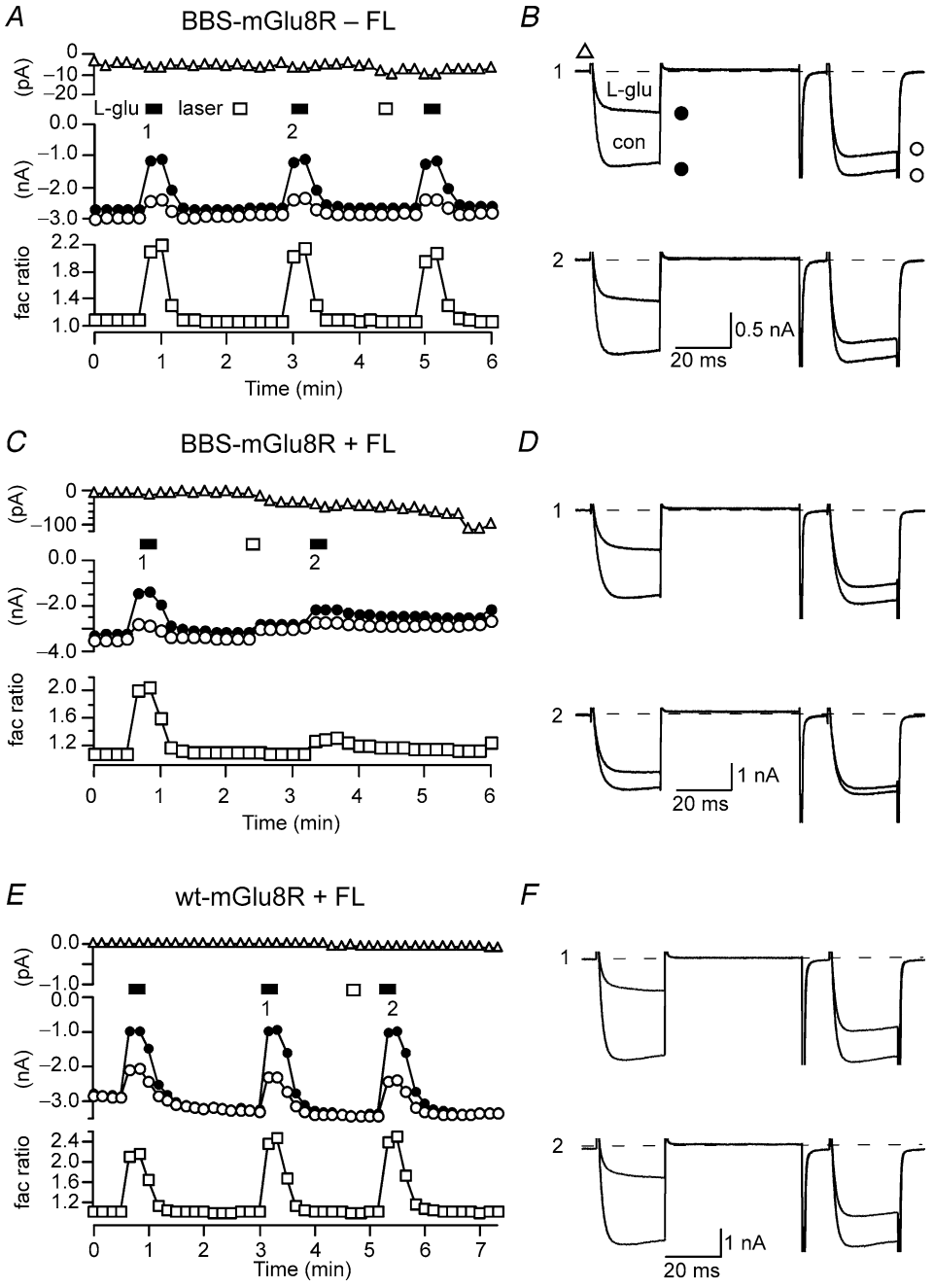

Figure 4. Laser illumination accelerated the rate of FALI
A, C and *E,* time course of the holding current (upper), I_{Ca} amplitudes (centre) and facilitation ratio (lower) for BBS–mGluR8a-expressing neurons in the absence (*A*) or presence (*C*) of FL–BTX labelling and for wt-mGluR8a-expressing neurons in the presence of FL–BTX application (*E*). The measurement of the holding current, the prepulse and postpulse I_{Ca} and facilitation ratio were as described in Fig. 2. *B, D* and *F*, superimposed I_{Ca} traces evoked with the double-pulse voltage protocol in the absence or presence of L-Glu (100 μM) from BBS–mGluR8a-expressing neurons in the absence (*B*) or presence of FL–BTX labelling (*D*) and wt-mGluR8a-expressing neurons in the presence of FL–BTX application (*F*). The upper panel (1) and lower panel (2) represent the prepulse I_{Ca} inhibition before and after illumination, respectively.

2.33 ± 0.11 to 1.41 ± 0.06 (Fig. 5*D*; $n = 19$; $P < 0.05$). The effect of decreasing illumination duration to 5 s was also examined. Effects on mean basal prepulse I_{Ca} amplitude (Fig. 5*A*) and holding current (Fig. 5*B*) were indistinguishable ($P > 0.05$) from the 10 s values. However, mean agonist-mediated prepulse I_{Ca} inhibition was 0.61 ± 0.11 ($n = 7$; Fig. 5*C*) of preillumination levels, a value significantly ($P < 0.05$) different from that produced by longer laser exposure. Thus, FALI disruption of mGluR8a-mediated I_{Ca} modulation was efficiently initiated by short exposures (5–10 s) of laser light delivered from an optical fibre. The magnitude of FALI was proportional to the duration of illumination. Ten seconds of laser light produced an effect (normalized agonist-mediated prepulse I_{Ca} inhibition) equivalent to 6 min of wide-field exposure.

To gain mechanistic insights into FALI, the effect of NaN_3 (10 mM added to both intracellular and extracellular solutions), a $^1O_2$ quencher, was examined. Inclusion of NaN_3 in the solutions did not affect preillumination prepulse I_{Ca} inhibition (mean inhibition $53 \pm 3\%$, $n = 7$, $P > 0.05$ compared with control). In the presence of NaN_3, laser illumination (10 s) still attenuated agonist-mediated prepulse I_{Ca} inhibition to 0.74 ± 0.04 ($n = 6$; Fig. 5*C*, grey bar; $P < 0.05$ compared with no fluorophore) of preillumination levels. However, the inhibition was less than the attenuation observed in the absence of NaN_3 (cf. 0.4, $P < 0.01$) supporting a role for $^1O_2$ generation in mediating the effects of FALI (Tour *et al.* 2003; Tanabe *et al.* 2005). We also examined the relationship between direct effects of FALI on N-type Ca^{2+} channels and agonist-mediated modulation parameters (Fig. 6). In Fig. 6*A*, normalized agonist-mediated prepulse I_{Ca} inhibition was plotted *versus basal* prepulse I_{Ca} inhibition produced by laser illumination of 5 s (open circles) or 10 s (filled circles) duration. Agonist-mediated and direct effects of FALI were significantly correlated (Pearson, $r^2 = 0.73$, $P < 0.0001$). A similar comparison of agonist-induced facilitation ratio *versus* laser-mediated direct effects on prepulse I_{Ca} (Fig. 6*B*) also produced a significant correlation (Pearson, $r^2 = 0.54$, $P < 0.0001$).

Time course of FALI-induced changes in I_{Ca} modulation

To assess the time course of FALI onset, neurons were exposed to laser illumination (10 s) during agonist exposure. Figure 7*A* illustrates persistent I_{Ca} inhibition by prolonged agonist (L-Glu, 100 μM; open bars) application to BBS–mGluR8s-expressing neurons. In control cells (absence of FL–BTX), during 5 min of agonist application there was a slight, gradual decrease in prepulse I_{Ca} inhibition (filled circles) and facilitation ratio (open squares). Similar to episodic agonist application (Fig. 4*A*), laser illumination (open bar) did not produce overt changes in I_{Ca} modulation. Upon removal of agonist, I_{Ca} quickly returned to the preinhibition level. In the cells

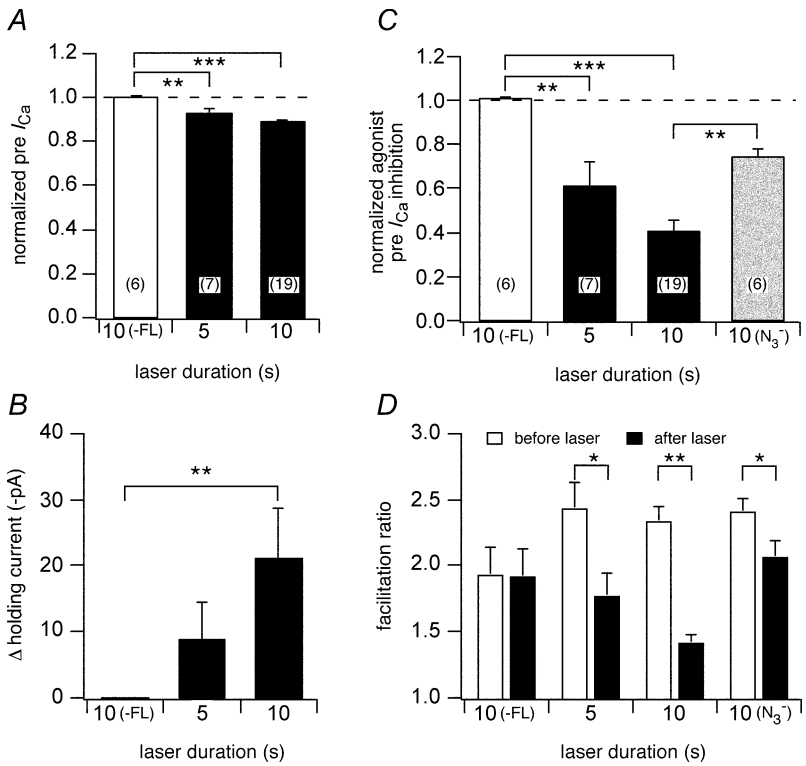

Figure 5. Laser illumination attenuated mGluR8a-mediated I_{Ca} modulation in FL–BTX labelled neurons, probably via generation of singlet oxygen
The effect of 5 and 10 s laser illumination on normalized prepulse I_{Ca} (*A*), holding current (*B*), L-Glu (100 μM)-induced prepulse I_{Ca} inhibition (*C*) and facilitation ratio (*D*), in the absence (open bars) or presence (filled bars) of FL–BTX labelling in BBS–mGluR8a-expressing neurons. The grey bar indicates the presence of the singlet oxygen quencher NaN_3 (10 mM) in the extracellular and intracellular solutions. The measurement of the holding current, the prepulse I_{Ca}, normalized agonist-induced inhibition and facilitation ratio were as described in Fig. 3. $^*P < 0.05$, $^{**}P < 0.01$, $^{***}P < 0.001$ compared with the control groups.

labelled with FL–BTX, 10 s laser illumination produced complex effects (Fig. 7*B*). The prepulse I_{Ca} increased (filled circles), the postpulse I_{Ca} decreased (filled circles) and the facilitation ratio (open squares) decreased with a relatively prolonged time course. Mean agonist-mediated prepulse and postpulse I_{Ca} inhibitions prior to and after illumination were similar for episodic (see Figs 4 and 5) and continuous agonist application except for a small but significantly ($P < 0.05$) larger postpulse I_{Ca} inhibition during continuous agonist application (data not shown). Basal and agonist facilitation ratios prior to or after illumination were similar regardless of whether agonist was present during laser illumination (Fig. 7*C*). The time course of I_{Ca} modulation was analysed by plotting the relaxation of the mean normalized facilitation ratio ($n = 7$) following laser illumination (Fig. 7*D*). Facilitation ratio was normalized by subtracting the steady-state component (~100 s following illumination) and dividing the facilitation ratio by the first value acquired following illumination. The relaxation was well fitted by a single exponential function (continuous line) with a τ of 12.4 ± 3 s (95% confidence interval) using non-linear least-squares regression. As the half-life of $^1O_2$ is 5–6 orders of magnitudes shorter than this, the decreases in I_{Ca} modulation occurring after laser illumination might result from 'dark reactions' (Davies, 2003), e.g. effects subsequent to inactivation of an enzyme, or relaxations in protein conformation following FALI-induced modification, e.g. unbinding of $G\beta\gamma$ from the Ca^{2+} channel following inactivation of a GPCR.

Disruption of I_{Ca} modulation with non-GPCR constructs

The previous data demonstrate that mGluR8a-mediated I_{Ca} modulation was disrupted by FALI while producing minimal direct effects on Ca^{2+} channels and membrane integrity. The proximity of the bound fluorophore to the agonist binding site made mGluR8a the most likely target for inactivation. To test whether such proximity was required for FALI disruption of I_{Ca} modulation, two BBS-tagged non-GPCR constructs were expressed and the modulation of I_{Ca} by natively expressed α_2-adrenoceptors (α_2-AR) were examined. The first construct, BBS–$Na_V\beta2$, was made by inserting a BBS into the extracellular N-terminus of the Na^+ channel $\beta2$ subunit ($Na_V\beta2$). $Na_V\beta2$, an accessory subunit of voltage-gated Na_V α-subunits, is predicted to have single transmembrane domain and extracellular Ig domain (McCormick *et al.* 1998). The second construct, 5-HT_3R–2BBS, has two tandem copies of the BBS (although ligand binding studies suggest that only one site is functional; D. Lovinger, personal communication) inserted into the extracellular C-terminus of 5-HT_3R, a ligand-gated ion channel. Both constructs produced prominent rim-like fluorescence when expressed in HEK 293 cells following incubation with fluorophore-tagged BTX (data not shown), indicating successful trafficking of proteins to the plasma membrane.

In control neurons (uninjected, no BTX), application of noradrenaline (NA; 10 μM) produced robust voltage-dependent I_{Ca} inhibition (Fig. 8*A*, filled bar;

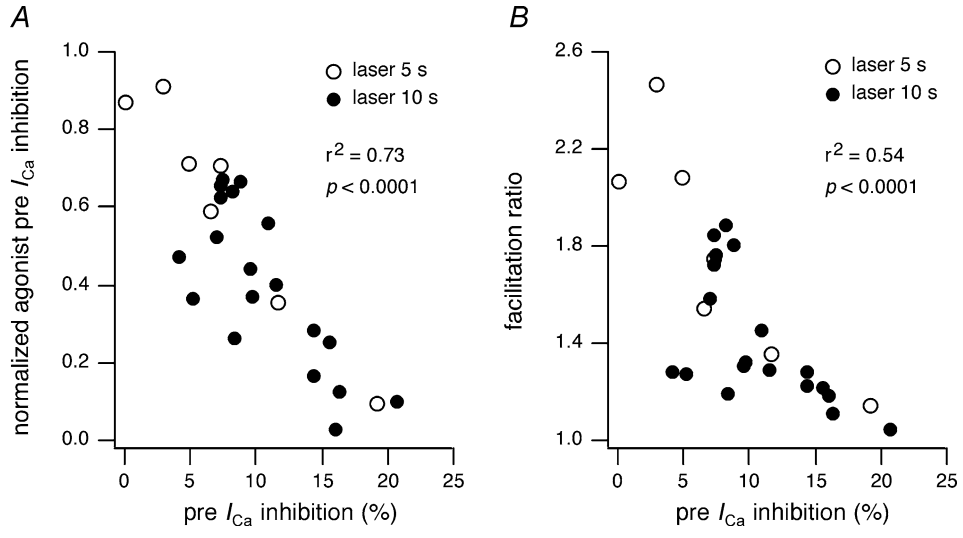

Figure 6. Correlation between agonist-mediated and direct effects of FALI
A, the normalized agonist-induced prepulse I_{Ca} inhibition after 5 s (○) or 10 s (●) was plotted *versus* laser-induced basal prepulse I_{Ca} inhibition. The basal prepulse I_{Ca} inhibition was calculated as the percentage change of the current after laser illumination. *B*, the facilitation ratio was plotted *versus* laser-induced basal prepulse I_{Ca} inhibition.

prepulse I_{Ca} inhibition of 53 ± 3%, $n = 4$) as previously documented (e.g. Ikeda, 1996). Laser illumination (10 s; Fig. 8*A*, open bar) produced no overt changes in I_{Ca} (Fig. 8*D*, open bar) or holding potential (data not shown) and had no significant effect on I_{Ca} modulation during subsequent agonist applications (prepulse I_{Ca} inhibition of 48 ± 7%, $n = 3$; Fig. 8*E*, open bar; facilitation ratio shown in Fig. 8*F*, leftmost bars). For BBS–$Na_V\beta 2$-expressing neurons incubated with FL–BTX, NA-induced prepulse I_{Ca} inhibition was similar to control neurons (54 ± 5%, $n = 3$). Unexpectedly, 10 s of laser illumination (Fig. 8*B*, open bar) significantly attenuated subsequent NA-mediated I_{Ca} modulation (Fig. 8*B*, *E* and *F*). Prepulse I_{Ca} inhibition was reduced to 0.20 ± 0.12 ($n = 4$) of preillumination values (Fig. 8*E*) and the facilitation ratio greatly attenuated (Fig. 8*F*). A variable effect on basal prepulse I_{Ca} amplitude was also noted (Fig. 8*D*, filled bar). Similar results were obtained with neurons expressing 5-HT_3R–2BBS and labelled with FL–BTX. Again, NA-induced prepulse I_{Ca} inhibition was unaffected prior to illumination (47 ± 5%, $n = 5$; Fig. 8*C*). However, following laser illumination (Fig. 8*C*, open bar), mean prepulse I_{Ca} inhibition fell to 0.35 ± 0.09 ($n = 3$) of preillumination values (Fig. 8*E*) and facilitation ratio was attenuated (Fig. 8*F*, rightmost bars). These data demonstrate the fluorophore labelling of proteins with no obvious relationship to the GPCR-Ca^{2+} channel signalling pathway can disrupt I_{Ca} modulation following laser illumination.

FALI effects on receptor-independent I_{Ca} modulation

Given the above results, we examined whether FALI disrupts receptor-independent I_{Ca} modulation.

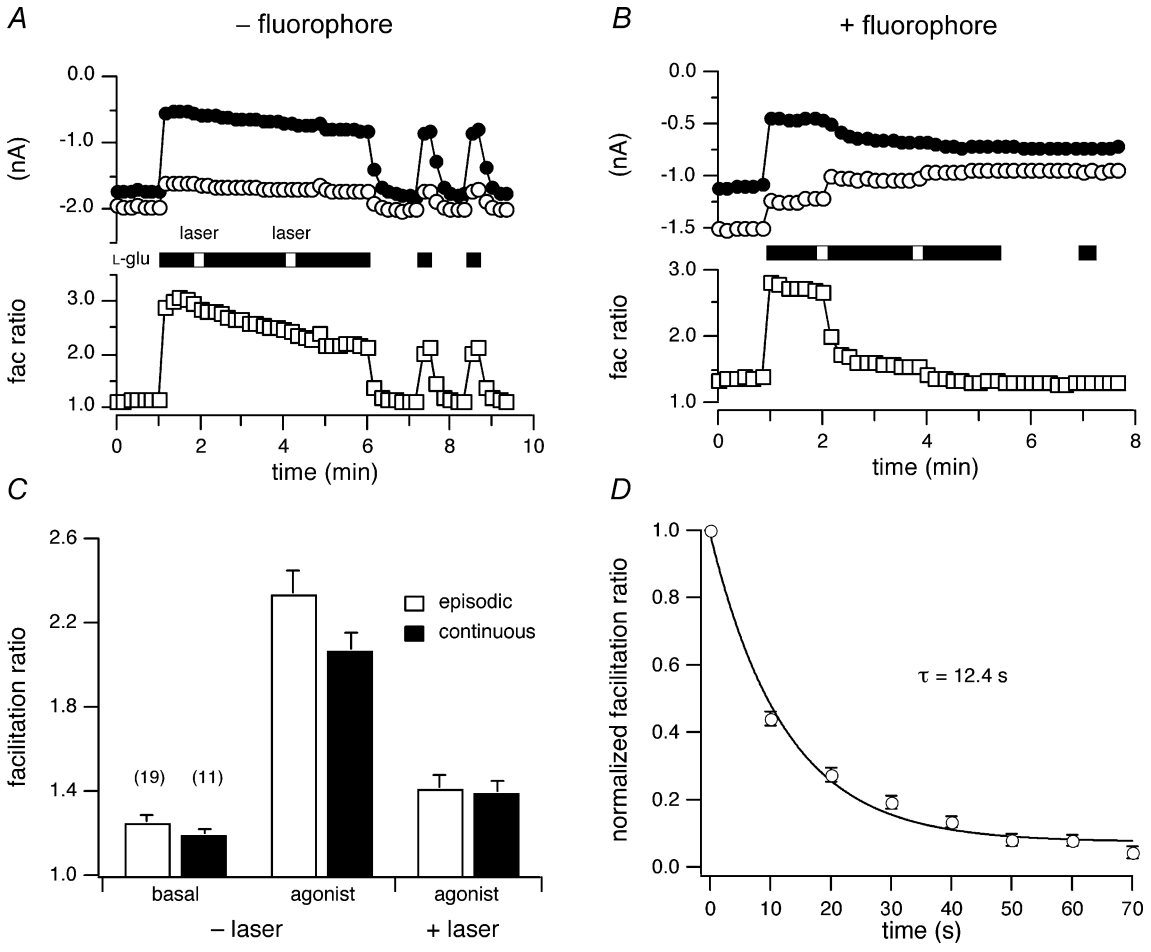

Figure 7. Time course of FALI-induced changes in I_{Ca} inhibition
A and *B*, time courses of the I_{Ca} amplitudes (upper) and facilitation ratio (lower) for BBS–mGluR8a-expressing neurons in the absence (*A*) or presence of FL–BTX labelling (*B*). *C*, the effect of episodic (*open bars*) and continuous (*filled bars*) laser illumination on facilitation ratio. *D*, mean ± S.E.M. ($n = 6$–7) normalized facilitation ratios were plotted *versus* time following 10 s illumination. Facilitation ratio was normalized by subtracting the steady-state component and dividing the facilitation ratio by the first value acquired following illumination. The continuous line represents the best fit to a single exponential function obtained using non-linear regression.

Voltage-dependent I_{Ca} modulation, analogous to that produced by agonist stimulation of GPCRs, can be elicited by introducing non-hydrolysable GTP analogues into the neuron via the patch electrode (Ikeda, 1996). Non-hydrolysable GTP analogues bind to the Gα subunits during basal GDP–GTP exchange thereby trapping Gα in an active conformation and constitutively modulating I_{Ca} (presumably via G$\beta\gamma$). This form of I_{Ca} modulation by-passes GPCR activation and thus reduces the signalling pathway to two principal components: heterotrimeric G-protein and N-type Ca^{2+} channels. For this purpose, 5-HT_3R–2BBS was expressed in the SCG neurons and labelled with FL–BTX and guanylyl imidophosphate, Gpp(NH)p, a non-hydrolysable GTP analogue, added to the pipette solution (0.5 mM). After the cell membrane was broken to attain the whole-cell configuration (Fig. 9*B*, trace '1'), prepulse I_{Ca} gradually decreased (Fig. 9*A*, filled circles) and the facilitation ratio increased (open squares) mimicking receptor-mediated voltage-dependent I_{Ca} inhibition (Fig. 9*B*, trace '2'). The modulated I_{Ca} reached a plateau 2–8 min after patch rupture attaining facilitation ratios between 2 and 3.7. At this time, the neuron was illuminated with the laser (10 s, Fig. 9*A*, open bars). There was an immediate *decrease* in postpulse I_{Ca} followed by a slowly developing *increase* in prepulse I_{Ca} (Fig. 9*B*, trace '3') resulting in a decrease in mean facilitation ratio (Fig. 9*D*, filled bar). The time course of change in the mean normalized facilitation ratio (Fig. 9*C*, normalized as in Fig. 7*D*) that was well fitted by a single exponential function with a $\tau = 24.9 \pm 6.7$ s (95% confidence interval). These data demonstrate that FALI can alter voltage-dependent I_{Ca}

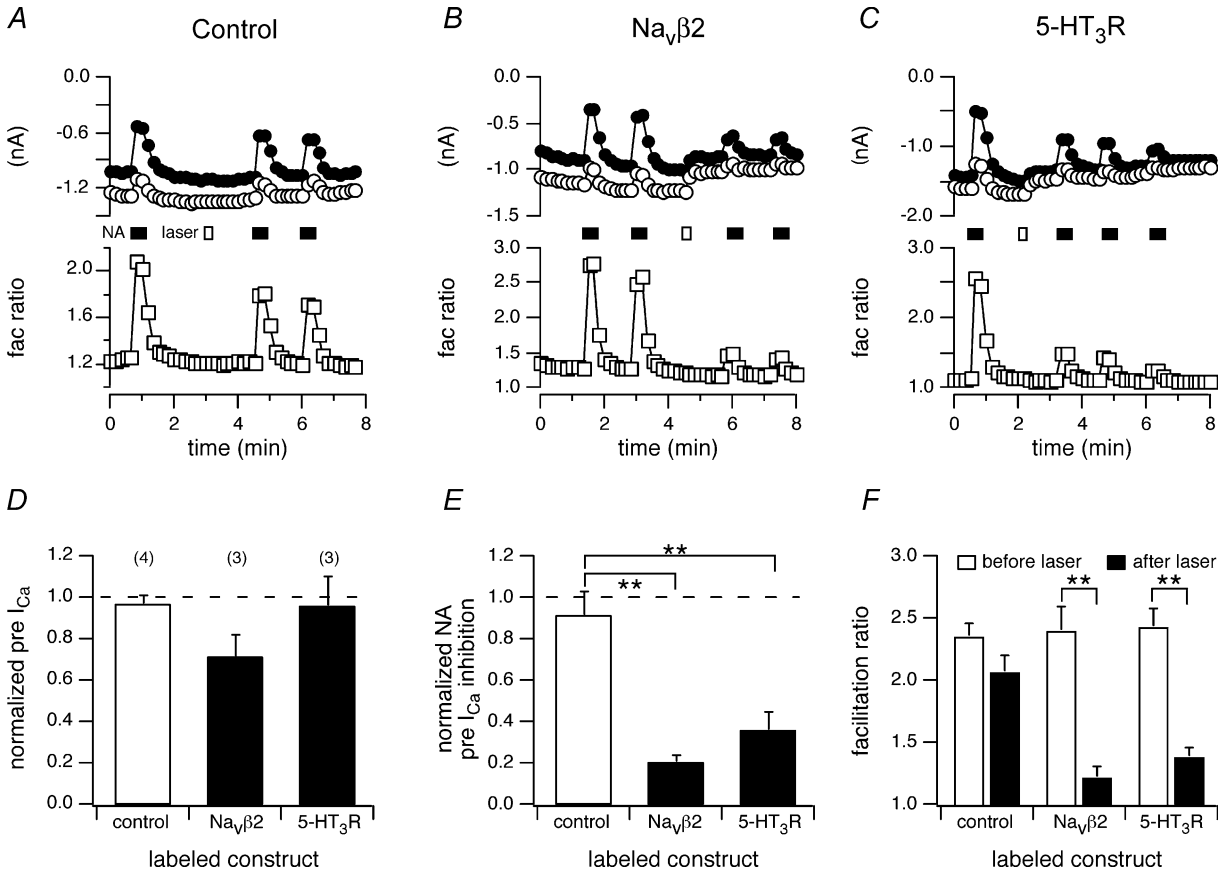

Figure 8. Laser illumination-attenuated noradrenaline-induced I_{Ca} modulation in BBS–Na$_V\beta$2- and 5-HT$_3$R–2BBS-expressing neurons labelled with FL–BTX

A, B and *C,* time courses of the I_{Ca} amplitudes for control (*A*), FL–BTX labelling, BBS–Na$_V\beta$2-expressing (*B*) and FL–BTX labelling, 5-HT_3R-expressing (*C*) neurons. I_{Ca} amplitude was measured 10 ms after initiation of the test pulse (+10 mV). The filled bars indicate 10 s laser illumination and the open bars indicate applications of noradrenaline (NA, 10 μM). *D, E* and *F*, the effect of 10 s laser illumination on normalized basal prepulse I_{Ca} amplitude (*D*), NA-induced I_{Ca} inhibition (*E*) and facilitation ratio in the absence (open bars) or presence (filled bars) of FL–BTX labelling in neurons expressing the indicated construct. The measurement of the prepulse I_{Ca}, normalized agonist-induced inhibition and facilitation ratio were as described in Fig. 3. $^{**}P < 0.01$, $^{***}P < 0.001$ compared with the control groups.

modulation in the absence of receptor labelling and activation.

Discussion

In the present study, we demonstrate disruption of mGluR8a-mediated modulation of N-type Ca^{2+} channels in sympathetic neurons by illumination of FL–BTX-labelled receptors. To our knowledge, this is the first study to examine GPCR coupling to an effector using FALI. Exposure of neurons expressing BBS–mGluR8a incubated with FL–BTX to either episcopic wide-field illumination or diascopic laser illumination delivered via an optical fibre attenuated voltage-dependent I_{Ca} modulation mediated by mGluR8a agonists (L-AP4 or L-Glu). The latter method produced significant inactivation on the second time scale even with minimal laser power. The process appeared relatively specific with minimal direct effects on I_{Ca} amplitude and holding current (an indicator of plasma membrane integrity). Facilitation ratio, a parameter used to assess G$\beta\gamma$-mediated voltage-dependent modulation, was decreased following FALI supporting specific interruption of this well-studied signalling pathway. Inclusion of N_3^-, a collision quencher of $^1O_2$, reduced the magnitude of FALI-mediated effects supporting a role for ROS. Although these results are consistent with inactivation of mGluR8a, the intended target,

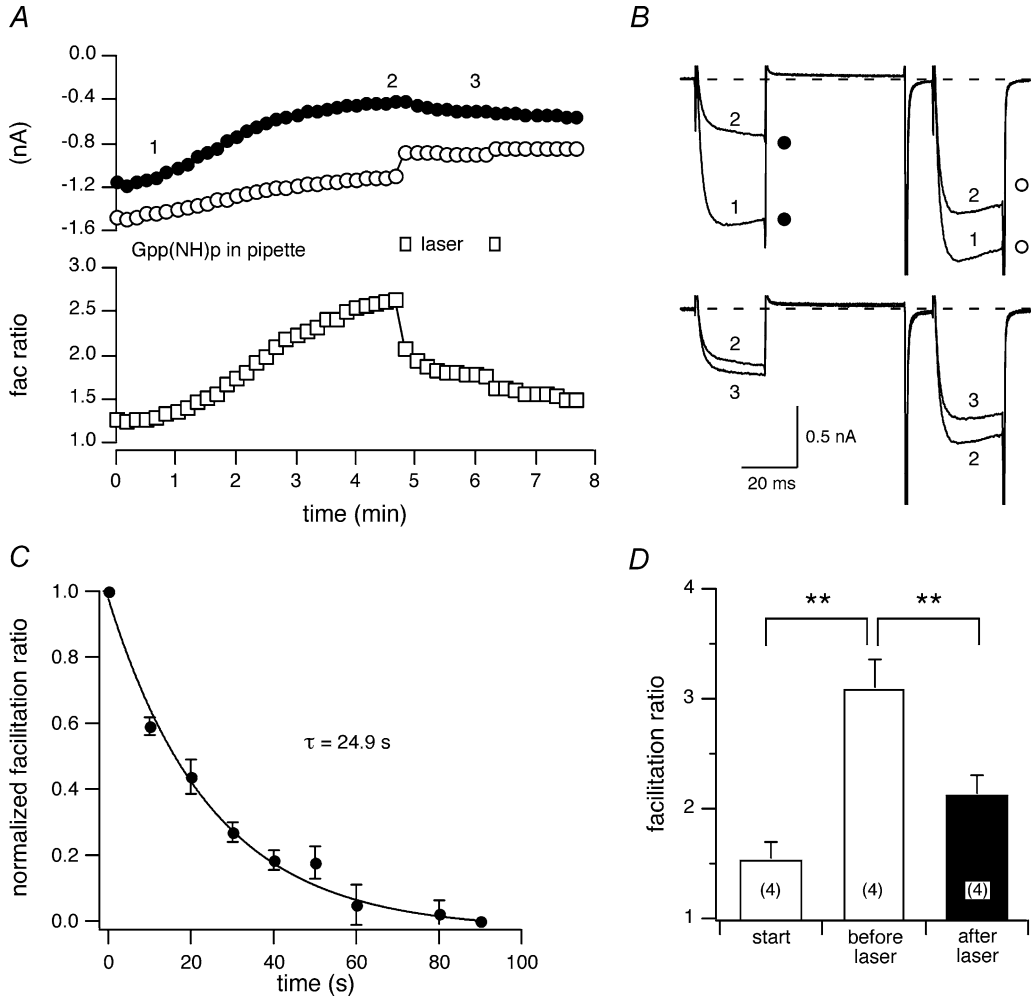

Figure 9. The effect of laser illumination on GPCR-independent I_{Ca} modulation
A, time courses of I_{Ca} amplitudes for FL–BTX-labelled 5-HT_3R–2BBS-expressing neurons. Guanylyl imidophosphate (Gpp(NH)p, 0.5 (mM) was included in the pipette solution. The open bars indicate 10 s laser illumination. *B,* superimposed I_{Ca} traces at the time immediately following rupture of the cell membrane (1), steady-state modulation (2) and after laser illumination (3). *C*, mean ± S.E.M. ($n = 4$) normalized facilitation ratios were plotted *versus* time following 10 s of illumination. The normalization of facilitation ratio was as described in Fig. 7*D*. The continuous line represents the best fit to a single exponential function obtained using non-linear regression. *D*, the effect of intracellular Gpp(NH)p and 10 s laser illumination on the facilitation ratio. $^{**}P < 0.01$.

two further findings confound this interpretation. First, similar effects on a natively expressed signalling pathway, α_2-AR-mediated I_{Ca} modulation, were obtained with non-GPCR-labelled constructs ($Na_V\beta2$ and 5-HT_3R). Second, receptor-independent voltage-dependent I_{Ca} modulation was also attenuated by FALI. Thus, caution when interpreting the mechanism of FALI-mediated effects is warranted.

In these experiments, we took advantage of a recently introduced technique (Sekine-Aizawa & Huganir, 2004; McCann *et al.* 2005) to examine a novel methodology for conducting FALI experiments, i.e. the use of fluorophore-labelled BTX bound to a genetically introduced BBS. Compared with other methodologies, advantages of the BTX–BBS system are: (1) the small ligand size (74 residues) should facilitate FALI by increasing fluorophore proximity to the targeted protein; (2) several fluorophore-conjugated BTXs are commercially available; (3) the BBS tag is small (13 residues), easily introduced into cDNA and should impact protein structure less than larger domains used for FALI such as EGFP (Rajfur *et al.* 2002; Tanabe *et al.* 2005) and the FKBP12 tag (Marks *et al.* 2004); and (4) FL–BTX binds to the BBS specifically and with high affinity thereby overcoming potential non-specific binding as has been reported for biarsenical dyes binding to tetracysteine motifs (Stroffekova *et al.* 2001; Tour *et al.* 2003). Disadvantages include: (1) BTX is not membrane permeable thus restricting use to surface epitopes or requiring a technique such as microinjection for introduction into the cytosol; (2) in general, native proteins cannot be targeted thus requiring genetic introduction and heterologous expression; and (3) in cells with nicotinic acetylcholine receptor subunit compositions that bind BTX with high affinity, specificity would be compromised. In regard to the latter concern, SCG neurons are reported to bind BTX, but in a rapidly reversible manner (Cuevas *et al.* 2000) that did not impact on the current studies (Fig. 4*E* and *F*). Our results indicate that the BTX–BBS system is a useful addition to the modalities currently used for FALI experiments.

An unexpected finding was the apparent collateral or long-range FALI effects on non-targeted proteins. These effects manifested in three ways. First, direct effects on the Ca^{2+} channel, as determined from decreases in basal I_{Ca} amplitude, were observed when BBS–mGluR8 was the labelled protein. Moreover, these effects were highly correlated with effects on I_{Ca} modulation (Fig. 6) suggesting that decreasing illumination power would not decrease collateral effects without impacting on FALI efficacy on I_{Ca} modulation. Second, labelling non-GPCR proteins without overt relationship to GPCR signalling pathways resulted in disruption of α_2-AR-mediated I_{Ca} modulation establishing that non-labelled components of the signalling pathway serve as potential targets of FALI (Fig. 8). Third, GPCR-independent voltage-dependent I_{Ca} modulation was affected by FALI proving that elements downstream from GPCR activation were modified (Fig. 9). How might these collateral effects arise? FALI via illumination of fluorescein is thought to occur through the production of $^1O_2$ and subsequent damage to nearby amino acids. The estimated half-maximal radius for fluorescein-mediated FALI is ~4 nm (Beck *et al.* 2002) and is believed to be determined by the distance over which $^1O_2$ diffuses before encountering a reactive molecule. As the inserted BBS was presumably close to the mGluR8a ligand binding site (extrapolated from the high resolution structure of mGluR1; Kunishima *et al.* 2000), it was reasonable to assume that the mGluR8a ligand binding domain would be the most accessible target in experiments employing BBS–mGluR8a. Indeed, the results are consistent with a preferential decrease in mGluR8a *versus* Ca^{2+} channel function although other interpretations are possible. A possible explanation for collateral effects are crowding of fluorescein-tagged proteins in the plasma membrane from high levels of expression bringing targets such as the Ca^{2+} channel (or even the G-protein subunits although these are minimally separated from the fluorophore by the plasma membrane, ~7 nm) within the sphere of $^1O_2$ influence. Given this scenario, decreasing BBS–mGluR8a expression should increase specificity. However, our initial experiments indicated that in the absence of visible labelling by FL–BTX, little disruption of I_{Ca} modulation was observed following illumination despite sufficient receptor expression to produce robust modulation (data not shown). The disruption of endogenous α_2-AR modulation following expression of the non-GPCR-labelled proteins, 5-HT_3R and $Na_V\beta2$ (Fig. 8), supports the idea of crowding and definitively proves that collateral FALI effects can occur from proteins outside the known signalling complex under study. It should be noted that even under this circumstance, basal I_{Ca} amplitude was minimally affected and thus global inactivation of plasma membrane proteins did not occur. Finally, the effects of FALI on Gpp(NH)p-mediated I_{Ca} modulation confirm that targets other than GPCRs can be affected since this form of modulation is independent of receptor stimulation.

Although collateral damage of FALI was observed here and by others (Hauptschein *et al.* 2005), many previous studies of CALI/FALI have concluded that the phenomenon is highly spatially restricted and hence specific for the targeted protein (Tour *et al.* 2003; Marks *et al.* 2004; Tanabe *et al.* 2005). How do we reconcile these findings with those reported here? CALI, using malachite green as the chromophore, probably inactivates proteins through the generation of hydroxyl radicals, a ROS with a much shorter half-life than $^1O_2$ and accordingly shorter range of action (Liao *et al.* 1994; Eustace & Jay, 2003). Hence specificity may

be better in this case although disadvantages exist (e.g. limited solubility and a requirement for high intensity pulsed laser) that have limited adoption of this modality. Other studies (Linden *et al.* 1992; Beck *et al.* 2002) have determined specificity with proteins in solution, a condition not equivalent to a plasma membrane delimited signalling pathway. It is possible that the efficacy of FALI effects on mGluR8 is not great thus requiring higher levels of expression (e.g. more receptors than G-proteins) that contribute to collateral effects. Such limited efficacy could arise from incomplete labelling (e.g. hidden epitopes, a population of unlabelled BTX), receptor reserve (i.e. a non-linear relationship between receptor inactivation and I_{Ca} modulation), or unusual resistance of mGluR8-$^1O_2$-mediated damage. Finally, it should be noted that the signalling pathway examined is probably spatially compact and thus susceptible to collateral effects and the methods used sufficiently sensitive to detect even modest changes in Ca^{2+} channel function.

Improving the efficacy of FALI provides a means of spatially restricting effects by allowing lowered expression levels of the tagged protein, decreased illumination power, or the inclusion of quenchers in the reaction. We speculate that FALI efficacy could be increased by optimizing the fluorophore. Fluorescein, although possessing a high quantum yield for photon emission ($\sim$0.9) and hence bright fluorescence, has a low quantum yield for $^1O_2$ generation ($\sim$0.03), the proposed mediator of FALI effects (Devanathan *et al.* 1990). The efficient decay from the excited singlet to ground state (and resulting photon emission) occurs at the expense of intersystem crossing to the excited triplet state that results in $^1O_2$ generation. In addition, fluorescein rapidly photobleaches thus terminating $^1O_2$ generation. Halogenation of fluorescein yields compounds with decreased fluorescence but increased quantum yield for $^1O_2$ generation and greater resistance to photobleaching. For example, eosin (tetrabromofluorescein) has a $^1O_2$ quantum yield $\sim$19 times greater than fluorescein and is more resistant to photobleaching (Deerinck *et al.* 1994).

In conclusion, our results demonstrate the GPCR signalling to N-type Ca^{2+} channels in neurons can be acutely disrupted using FALI. However, collateral effects on non-targeted proteins were observed and thus caution is warranted when interpreting FALI effects as the radius of protein inactivation may be greater than previously realized.

References

Beck S, Sakurai T, Eustace BK, Beste G, Schier R, Rudert F & Jay DG (2002). Fluorophore-assisted light inactivation: a high-throughput tool for direct target validation of proteins. *Proteomics* **2**, 247–255.

Campbell RE, Tour O, Palmer AE, Steinbach PA, Baird GS, Zacharias DA & Tsien RY (2002). A monomeric red fluorescent protein. *Proc Natl Acad Sci U S A* **91**, 7877–7882.

Cuevas J, Roth AL & Berg DK (2000). Two distinct classes of functional α7-containing nicotinic receptor on rat superior cervical ganglion neurons. *J Physiol* **525**, 735–746.

Davies MJ (2003). Singlet oxygen-mediated damage to proteins and its consequences. *Biochem Biophys Res Commun* **305**, 761–770.

Deerinck TJ, Martone ME, Lev-Ram V, Green DP, Tsien RY, Spector DL, Huang S & Ellisman MH (1994). Fluorescence photooxidation with eosin: a method for high resolution immunolocalization and in situ hybridization detection for light and electron microscopy. *J Cell Biol* **126**, 901–910.

Devanathan S, Dahl TA, Midden WR & Neckers DC (1990). Readily available fluorescein isothiocyanate-conjugated antibodies can be easily converted into targeted phototoxic agents for antibacterial, antiviral and anticancer therapy. *Proc Natl Acad Sci U S A* **87**, 2980–2984.

Elmslie KS, Zhou W & Jones SW (1990). LHRH and GTP-γ-S modify calcium current activation in bullfrog sympathetic neurons. *Neuron* **5**, 75–80.

Eustace BK & Jay DG (2003). Fluorophore-assisted light inactivation for multiplex analysis of protein function in cellular processes. *Meth Enzymol* **360**, 649–660.

Guo J & Ikeda SR (2005). Coupling of metabotropic glutamate receptor 8 to N-type Ca^{2+} channels in rat sympathetic neurons. *Mol Pharmacol* **67**, 1840–1851.

Hauptschein RS, Sloan KE, Torella C, Moezzifard R, Giel-Moloney M, Zehetmeier C, Unger C, Ilag LL & Jay DG (2005). Functional proteomic screen identifies a modulating role for CD44 in death receptor-mediated apoptosis. *Cancer Res* **65**, 1887–1896.

Herlitze S, Garcia DE, Mackie K, Hille B, Scheuer T & Catterall WA (1996). Modulation of Ca^{2+} channels by G-protein $\beta\gamma$ subunits. *Nature* **380**, 258–262.

Horstkotte E, Schröder T, Niewöhner J, Thiel E, Jay DG & Henning SW (2005). Toward understanding the mechanism of chromophore-assisted laser inactivation – evidence for the primary photochemical steps. *Photochem Photobiol* **81**, 358–366.

Ikeda SR (1991). Double-pulse calcium channel current facilitation in adult rat sympathetic neurones. *J Physiol* **439**, 181–214.

Ikeda SR (1996). Voltage-dependent modulation of N-type calcium channels by G-protein $\beta\gamma$ subunits. *Nature* **380**, 255–258.

Ikeda SR (2004). Expression of G-protein signaling components in adult mammalian neurons by microinjection. *Meth Mol Biol* **259**, 167–181.

Ikeda SR & Dunlap K (1999). Voltage-dependent modulation of N-type calcium channels: role of G protein subunits. *Adv Second Messenger Phosphoprotein Res* **33**, 131–151.

Ikeda SR & Jeong SW (2004). Use of RGS-insensitive Gα subunits to study endogenous RGS protein action on G-protein modulation of N-type calcium channels in sympathetic neurons. *Meth Enzymol* **389**, 170–189.

Ikeda SR, Lovinger DM, McCool BA & Lewis DL (1995). Heterologous expression of metabotropic glutamate receptors in adult rat sympathetic neurons: subtype-specific coupling to ion channels. *Neuron* **14**, 1029–1038.

Jay DG (1988). Selective destruction of protein function by chromophore-assisted laser inactivation. *Proc Natl Acad Sci U S A* **85**, 5454–5458.

Kammermeier PJ & Ikeda SR (1999). Expression of RGS2 alters the coupling of metabotropic glutamate receptor 1a to M-type K^+ and N-type Ca^{2+} channels. *Neuron* **22**, 819–829.

Kniazeff J, Bessis AS, Maurel D, Ansanay H, Prezeau L & Pin JP (2004). Closed state of both binding domains of homodimeric mGlu receptors is required for full activity. *Nat Struct Mol Biol* **11**, 706–713.

Kunishima N, Shimada Y, Tsuji Y, Sato T, Yamamoto M, Kumasaka T, Nakanishi S, Jingami H & Morikawa K (2000). Structural basis of glutamate recognition by a dimeric metabotropic glutamate receptor. *Nature* **407**, 971–977.

Liao JC, Roider J & Jay DG (1994). Chromophore-assisted laser inactivation of proteins is mediated by the photogeneration of free radicals. *Proc Natl Acad Sci U S A* **91**, 2659–2663.

Linden KG, Liao JC & Jay DG (1992). Spatial specificity of chromophore assisted laser inactivation of protein function. *Biophys J* **61**, 956–962.

McCann CM, Bareyre FM, Lichtman JW & Sanes JR (2005). Peptide tags for labeling membrane proteins in live cells with multiple fluorophores. *Biotechniques* **38**, 945–952.

McCormick KA, Isom LL, Ragsdale D, Smith D, Scheuer T & Catterall WA (1998). Molecular determinants of Na^+ channel function in the extracellular domain of the β1 subunit. *J Biol Chem* **273**, 3954–3862.

Marks KM, Braun PD & Nolan GP (2004). A general approach for chemical labeling and rapid, spatially controlled protein inactivation. *Proc Natl Acad Sci U S A* **101**, 9982–9987.

Rajfur Z, Roy P, Otey C, Romer L & Jacobson K (2002). Dissecting the link between stress fibres and focal adhesions by CALI with EGFP fusion proteins. *Nat Cell Biol* **4**, 286–293.

Sekine-Aizawa Y & Huganir RL (2004). Imaging of receptor trafficking by using α-bungarotoxin-binding-site-tagged receptors. *Proc Natl Acad Sci U S A* **101**, 17114–17119.

Stroffekova K, Proenza C & Beam KG (2001). The protein-labeling reagent FLASH-EDT2 binds not only to CCXXCC motifs but also non-specifically to endogenous cysteine-rich proteins. *Pflugers Arch* **442**, 859–866.

Tanabe T, Oyamada M, Fujita K, Dai P, Tanaka H & Takamatsu T (2005). Multiphoton excitation-evoked chromophore-assisted laser inactivation using green fluorescent protein. *Nat Meth* **2**, 503–505.

Thomas M, Lu JL, Zhang C, Chen J & Kilbanoz AM (2005). Full deacylation of polyethylenimine dramatically boosts its gene delivery efficiency and specificity to mouse lung. *Proc Natl Acad Sci U S A* **102**, 5679–5684.

Tour O (2005). EGFP as your targeted 'hitman'. *Nat Meth* **2**, 491–492.

Tour O, Meijer RM, Zacharias DA, Adams SR & Tsien RY (2003). Genetically targeted chromophore-assisted light inactivation. *Nat Biotechnol* **21**, 1505–1508.

Acknowledgements

We would like to thank Dr David M. Lovinger (NIH/NIAAA, Rockville, MD, USA) for the 5-HT_3R–2BBS cDNA construct. We are grateful to Drs Geoffrey Schofield (Tulane University Medical School, New Orleans, LA, USA) and Ruquia Ahmed-Schofield (Xavier University, New Orleans, LA, USA) for supplying fully deacylated polyethylenimine. This research was supported by the Intramural Research Program of the NIH, National Institute on Alcohol Abuse and Alcoholism.